Free-Vibration Analysis and Material Constants Identification of Laminated Composite Sandwich Plates

C. R. Lee[1]; T. Y. Kam[2]; and S. J. Sun[3]

Abstract: Free vibration of symmetrically laminated composite sandwich plates with elastic edge restraints is studied via the Rayleigh–Ritz approach. The proposed Rayleigh–Ritz method is constructed on the basis of the layer-wise linear displacement theory. The accuracy of the method in predicting natural frequencies of composite sandwich plates with different boundary conditions is verified by the results reported in the literature or the experimental data obtained in this study. The proposed method is then applied to the material constant identification of free composite sandwich plates using the first six theoretical natural frequencies of the plates. In the identification process, trial material constants are used in the present method to predict the theoretical natural frequencies, a frequency discrepancy function is established to measure the sum of the squared differences between the experimental and theoretical natural frequencies, and a stochastic global minimization algorithm is used to search for the best estimates of the material constants by making the frequency discrepancy function a global minimum. Applications of the material constant identification technique are demonstrated by means of several examples.

DOI: 10.1061/(ASCE)0733-9399(2007)133:8(874)

CE Database subject headings: Composite materials; Sandwich panels; Plates; Vibration; Laminates.

Introduction

Recently, fiber-reinforced composite sandwich plates have been widely used in the aerospace, automobile, and ship building industries to fabricate high-performance structures. In general, attainment of actual behavioral predictions of composite sandwich plates depends on the correctness of the mathematical modeling and elastic constants of the plates. As is well known, composite structures fabricated using different methods or curing processes may possess different mechanical properties, and because of this, the material properties determined from the standard specimens tested in the laboratory, in general, may deviate from those of actual laminated composite structures. Since attainment of actual material constants is vital to integrity assessment of structures, determination of the mechanical properties of structures, especially composite plate structures, has thus become an important topic of research in recent years. For instance, Deobald and Gibson (1988) used a Rayleigh–Ritz/modal analysis technique to determine the elastic constants of composite plates with different boundary conditions. Castagnède et al. (1990) determined the elastic constants of thick composite plates via a quantitative ultrasonic approach. Fallstrom and Jonsson (1991) determined the material constants of anisotropic plates from the frequencies and mode shapes measured by a real-time television-holography system. Several researchers developed methods to identify structural stiffness matrices or the element bending stiffness of beam structures using measured natural frequencies and mode shapes (Berman and Nagy 1983; Kam and Lee 1994; Kam and Liu 1998). Wang and Kam (2001) developed a two-stage nondestructive evaluation method in which strains and/or displacements obtained from static testing of laminated composite plates clamped at the edges are used to identify the elastic constants of the plates. Recently, a number of researchers have used experimental natural frequencies to identify the elastic constants of laminated composite plates with free boundary conditions (Moussu and Nivoit 1993; Sol et al. 1997; Qian et al. 1997; Hwang and Chang 2000). For instance, Moussu and Nivoit (1993) used the method of superposition to determine the elastic constants of free orthotropic plates from measured natural frequencies. Sol et al. (1997) used the method of Bayesian estimation to study the identification of elastic constants from experimental natural frequencies of free rectangular orthotropic plates.

The free vibration of sandwich plates with regular boundary conditions such as simply supported or clamped edges has been studied by many researchers, and different methods have also been proposed to determine the modal characteristics of such plates (Ueng 1966; Watanabe et al. 1993; Masoud and Pierre 1999; Nayak et al. 2002). Regarding material constant identification of sandwich plates, although it is an important topic of research, there has been only limit work devoted to this area. For instance, Thwaites and Clark (1995) used elastic waves to detect and identify core damage and skin delamination of honeycomb sandwich plates. Saito et al. (1997) presented a method established on the basis of Timoshenko beam theory to deal with parameter identification of aluminum honeycomb sandwich panels. If realistic mechanical behaviors of laminated composite sandwich plates are to be predicted, more attention should be drawn to the area of material constant identification of plates and the capa-

[1]Associate Professor, Aeronautic and Mechanical Engineering Dept., Chinese Air Force Academy, P.O. Box 90277-11 Kang-Shan, Kaohsiung County, Taiwan, Republic of China.

[2]Professor, Mechanical Engineering Dept., National Chiao Tung Univ., Hsin Chu 300, Taiwan, Republic of China (corresponding author). E-mail: tykam@mail.nctu.edu.tw

[3]Research Assistant, Mechanical Engineering Dept., National Chiao Tung Univ., Hsin Chu 300, Taiwan, Republic of China.

Note. Associate Editor: Joel P. Conte. Discussion open until January 1, 2008. Separate discussions must be submitted for individual papers. To extend the closing date by one month, a written request must be filed with the ASCE Managing Editor. The manuscript for this paper was submitted for review and possible publication on April 24, 2006; approved on March 7, 2007. This paper is part of the ***Journal of Engineering Mechanics***, Vol. 133, No. 8, August 1, 2007. ©ASCE, ISSN 0733-9399/2007/8-874–886/$25.00.

J. Eng. Mech. 2007.133:874-886.

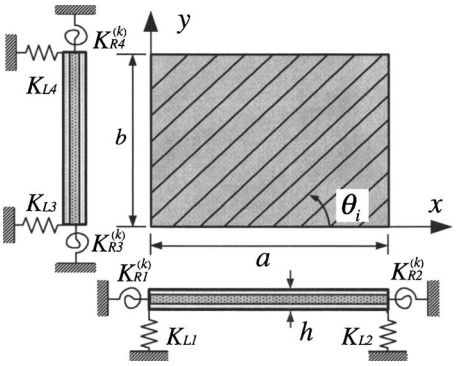

Fig. 1. Flexibly supported composite sandwich plate

bility of nondestructive evaluation techniques used in this area should be explored in depth.

In this paper, a method is established for free vibration analysis of symmetrically laminated composite sandwich plates restrained by flexible edge supports. A number of examples are given to demonstrate the accuracy of the present method in predicting the natural frequencies of symmetrically laminated composite sandwich plates with different boundary conditions. The present method is then applied to the material constant identification of laminated composite sandwich plates via the mixed numerical/experimental approach. The theoretical natural frequencies of a free laminated composite sandwich plate predicted by the present method using trial material constants, together with the measured natural frequencies of the plate, are used to construct the frequency discrepancy function, which measures the sum of the squared differences between the experimental and theoretical natural frequencies of the plate. The identification of the material constants of the sandwich plate is then formulated as a constrained minimization problem in which the material constants are determined by making the frequency discrepancy function a global minimum. The capability and efficiency of the identification method in estimating accurate material constants of laminated composite sandwich plates with different properties will be demonstrated by means of a number of examples.

Vibration Analysis of Composite Sandwich Plate

Consider the elastically restrained rectangular symmetrically laminated composite sandwich plate of area $a \times b$ and constant thickness h composed of two thin, laminated composite face sheets with thicknesses h_f at the top and bottom surfaces of a relatively thick core layer with thickness h_c, as shown in Fig. 1. The x and y coordinates of the plate are taken in the midplane of the plate. Herein, the layer-wise linear displacement theory (Mau 1973; Kam and Jan 1995) is used to determine the displacement field of the sandwich plate. The sandwich plate is divided into three layer groups in which the core, upper face sheet, and lower face sheet are numbered as Layer Groups 1, 2, and 3, respectively. The displacement components of the sandwich plate are assumed to be of the following forms:

$$w_0(x,y,t) = W(x,y)\sin \omega t, \quad \theta_x^{(k)}(x,y,t) = \Theta_x^{(k)}(x,y)\sin \omega t$$
$$\theta_y^{(k)}(x,y,t) = \Theta_y^{(k)}(x,y)\sin \omega t, \quad (k = 1\text{–}3) \tag{1}$$

where $w_0(x,y,t)$=vertical deflection at plate midplan; $\theta_x^{(k)}(x,y,t)$ and $\theta_y^{(k)}(x,y,t)$=rotations of cross sections perpendicular to the x and y axes, respectively, of the kth layer group; W=deflection function; $\Theta_x^{(k)}$ and $\Theta_y^{(k)}$=rotation functions; ω=angular frequency; and t=time. In Fig. 2, the displacement field of the core (Layer Group 1) is given as

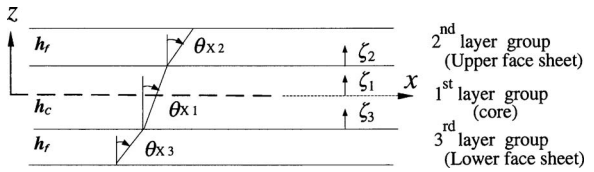

Fig. 2. Layer groups of laminated composite sandwich plate

$$u^{(1)}(x,y,z,t) = u_0(x,y,t) + \zeta^{(1)}\theta_x^{(1)}(x,y,t)$$
$$v^{(1)}(x,y,z,t) = v_0(x,y,t) + \zeta^{(1)}\theta_y^{(1)}(x,y,t) \tag{2}$$
$$w^{(1)}(x,y,z,t) = w_0(x,y,t)$$

where $u^{(1)}$ and $v^{(1)}$=in-plane displacements at any point in the x and y directions, respectively; u_0, v_0=in-plane displacements at the midplane; $w^{(1)}$=vertical displacement in the z direction; and $\zeta^{(1)}$=local coordinate in the thickness direction.

Similarly, the displacement fields of the upper face sheet (Layer Group 2) and lower face sheet (Layer Group 3) are given, respectively, as

Upper face sheet

$$u^{(2)}(x,y,z,t) = u^{(1)}\left(x,y,\frac{h_c}{2},t\right) + \zeta^{(2)}\theta_x^{(2)}(x,y,t)$$
$$v^{(2)}(x,y,z,t) = v^{(1)}\left(x,y,\frac{h_c}{2},t\right) + \zeta^{(2)}\theta_y^{(2)}(x,y,t) \tag{3a}$$
$$w^{(2)}(x,y,z,t) = w_0(x,y,t)$$

Lower face sheet

$$u^{(3)}(x,y,z,t) = u^{(1)}\left(x,y,\frac{-h_c}{2},t\right) + \zeta^{(3)}\theta_x^{(3)}(x,y,t)$$
$$v^{(3)}(x,y,z,t) = v^{(1)}\left(x,y,\frac{-h_c}{2},t\right) + \zeta^{(3)}\theta_y^{(3)}(x,y,t) \tag{3b}$$
$$w^{(3)}(x,y,z,t) = w_0(x,y,t)$$

where $\zeta^{(k)}$=local coordinate in the kth layer group. It is noted that for the symmetric sandwich plate, the cross-sectional rotations at Layer Groups 2 and 3 are the same, i.e., $\Theta_x^{(2)}(\xi,\eta) = \Theta_x^{(3)}(\xi,\eta)$ and $\Theta_y^{(2)}(\xi,\eta) = \Theta_y^{(3)}(\xi,\eta)$. Furthermore, for small deflection, u_0 and v_0 are negligible and can be discarded. Therefore, the independent displacement components reduce from 9 to 5. The strain–displacement relations for each layer group can be expressed in matrix form as

J. Eng. Mech. 2007.133:874-886.

$$\begin{Bmatrix} \varepsilon_x^{(k)} \\ \varepsilon_y^{(k)} \\ \gamma_{xy}^{(k)} \\ \gamma_{yz}^{(k)} \\ \gamma_{xz}^{(k)} \end{Bmatrix} = \begin{Bmatrix} \dfrac{\partial u^{(k)}}{\partial x} \\ \dfrac{\partial v^{(k)}}{\partial y} \\ \dfrac{\partial u^{(k)}}{\partial y} + \dfrac{\partial v^{(k)}}{\partial x} \\ \dfrac{\partial v^{(k)}}{\partial z} + \dfrac{\partial w^{(k)}}{\partial y} \\ \dfrac{\partial u^{(k)}}{\partial z} + \dfrac{\partial w^{(k)}}{\partial x} \end{Bmatrix} \tag{4}$$

where ε, γ=are normal and shear strains, respectively; and superscript (k) denotes layer group number. The stress–strain relations for the three layer groups in the global x–y–z coordinate system can be expressed in the following general form (Swanson 1997):

$$\begin{Bmatrix} \sigma_{xm}^{(k)} \\ \sigma_{ym}^{(k)} \\ \tau_{xym}^{(k)} \\ \tau_{yzm}^{(k)} \\ \tau_{xzm}^{(k)} \end{Bmatrix} = \begin{bmatrix} \bar{Q}_{11m}^{(k)} & \bar{Q}_{12m}^{(k)} & \bar{Q}_{16m}^{(k)} & 0 & 0 \\ \bar{Q}_{12m}^{(k)} & \bar{Q}_{22m}^{(k)} & \bar{Q}_{23m}^{(k)} & 0 & 0 \\ \bar{Q}_{16m}^{(k)} & \bar{Q}_{26m}^{(k)} & \bar{Q}_{66m}^{(k)} & 0 & 0 \\ 0 & 0 & 0 & \bar{Q}_{44m}^{(k)} & \bar{Q}_{45m}^{(k)} \\ 0 & 0 & 0 & \bar{Q}_{45m}^{(k)} & \bar{Q}_{55m}^{(k)} \end{bmatrix} \begin{Bmatrix} \varepsilon_{xm}^{(k)} \\ \varepsilon_{ym}^{(k)} \\ \gamma_{xym}^{(k)} \\ \gamma_{yzm}^{(k)} \\ \gamma_{xzm}^{(k)} \end{Bmatrix} \tag{5}$$

where σ, τ=normal and shear stresses, respectively; and $\bar{Q}_{ijm}^{(k)}$=transformed lamina stiffness coefficient, which depends on the material properties and fiber orientation of the mth lamina in the kth layer group. The relation between the transformed and untransformed lamina stiffness coefficients is expressed as

$$\bar{Q}_{11} = Q_{11}C^4 + 2(Q_{12} + 2Q_{66})C^2S^2 + Q_{22}S^4$$

$$\bar{Q}_{12} = (Q_{11} + Q_{22} - 4Q_{66})C^2S^2 + Q_{12}(C^4 + S^4)$$

$$\bar{Q}_{16} = (Q_{11} - Q_{12} - 2Q_{66})C^3S + (Q_{12} - Q_{22} + 2Q_{66})CS^3$$

$$\bar{Q}_{22} = Q_{11}S^4 + 2(Q_{12} + 2Q_{66})C^2S^2 + Q_{22}C^4$$

$$\bar{Q}_{26} = (Q_{11} - Q_{12} - 2Q_{66})CS^3 + (Q_{12} - Q_{22} + 2Q_{66})C^3S$$

$$\bar{Q}_{66} = (Q_{11} + Q_{22} - 2Q_{12} - 2Q_{66})C^2S^2 + Q_{66}(C^4 + S^4)$$

$$\bar{Q}_{44} = Q_{44}C^2 + Q_{55}S^2, \bar{Q}_{45} = (Q_{55} - Q_{44})CS$$

$$\bar{Q}_{55} = Q_{55}C^2 + Q_{44}S^2 \tag{6}$$

with

$$Q_{11} = \frac{E_1}{1 - \upsilon_{12}\upsilon_{21}}; \quad Q_{12} = \frac{\upsilon_{12}E_2}{1 - \upsilon_{12}\upsilon_{21}}; \quad Q_{22} = \frac{E_2}{1 - \upsilon_{12}\upsilon_{21}}$$

$$Q_{44} = G_{23}; \quad Q_{55} = G_{13}; \quad Q_{66} = G_{12}; \quad C = \cos\theta_i; \quad S = \sin\theta_i \tag{7}$$

where Q_{ij}=untransformed lamina stiffness coefficient; E_1, E_2=Young's moduli in the fiber and transverse directions, respectively; ν_{ij}=Poisson's ratio for transverse strain in the j direction when stressed in the i direction; G_{12}=in-plane shear modulus in the 1–2 plane; G_{13} and G_{23}=transverse shear moduli in the 1–3 and 2–3 planes, respectively; and θ_i=lamina fiber angle of the ith lamina. Herein, for the thin face sheets, the transverse shear effects are assumed to be so small that the transverse shear moduli (G_{13} and G_{23}) are treated the same as the in-plane shear modulus (G_{12}). For the core made of isotropic material, the independent elastic constants in Eq. (7) are Young's modulus E_c and Poisson's ratio ν_c. The strain energy U_P and kinetic energy T of the plate are expressed, respectively, as

$$U_P = \sum_{k=1}^{3} \int_{V^{(k)}} \frac{1}{2}\sigma^{(k)T}\varepsilon^{(k)}dV^{(k)} \tag{8}$$

and

$$T = \sum_{k=1}^{3} \frac{1}{2}\int_{V^{(k)}} \rho^{(k)}(\dot{u}^{(k)^2} + \dot{v}^{(k)^2} + \dot{w}^{(k)^2})dV^{(k)} \tag{9}$$

where $\rho^{(k)}$=material density; $V^{(k)}$=volume;
$\boldsymbol{\sigma}^{(k)T} = [\sigma_x^{(k)}, \sigma_y^{(k)}, \tau_{xy}^{(k)}, \tau_{yz}^{(k)}, \tau_{xz}^{(k)}]$=stress vector;
$\boldsymbol{\varepsilon}^{(k)T} = [\varepsilon_x^{(k)}, \varepsilon_y^{(k)}, \gamma_{xy}^{(k)}, \gamma_{yz}^{(k)}, \gamma_{xz}^{(k)}]$=strain vector, respectively; and $\dot{u}$, $\dot{v}$, and $\dot{w}$=velocities in the x, y, and z directions, respectively. After substituting the displacement equations and stress–strain relations into Eqs. (8) and (9) and performing the derivatives, the maximun strain energy U_{Pm} and kinetic energy T_m of the plate can be obtained by letting the terms of $\sin\omega t$ and $\cos\omega t$ be equal to 1. For the plate restrained by elastic edge supports, additional strain energy stored in the boundary springs exists. A general form for evaluating the maximum total strain energy of the flexible restraints, U_B, is written as

$$\begin{aligned} U_B = {} & \frac{K_{L1}}{2}\left[\int_0^b W^2 dy\right]_{x=0} + \frac{K_{L2}}{2}\left[\int_0^b W^2 dy\right]_{x=a} \\ & + \frac{K_{L3}}{2}\left[\int_0^a W^2 dx\right]_{y=0} + \frac{K_{L4}}{2}\left[\int_0^a W^2 dx\right]_{y=b} \\ & + \sum_{k=1}^{3}\left\{\frac{K_{R1}^{(k)}}{2}\left[\int_0^b \Theta_x^{(k)^2} dy\right]_{x=0} + \frac{K_{R2}^{(k)}}{2}\left[\int_0^b \Theta_x^{(k)^2} dy\right]_{x=a}\right. \\ & \left. + \frac{K_{R3}^{(k)}}{2}\left[\int_0^a \Theta_y^{(k)^2} dx\right]_{y=0} + \frac{K_{R4}^{(k)}}{2}\left[\int_0^a \Theta_y^{(k)^2} dx\right]_{y=b}\right\} \end{aligned} \tag{10}$$

where K_{Li}=spring constant intensity of the longitudinal spring at the ith edge; and $K_{Ri}^{(k)}$=spring constant intensity of the torsional spring at the kth layer group of the ith edge, respectively. The integrals in the brackets of the above equation are evaluated at the four edges of the plate. The total maximum strain energy of the flexibly supported plate is then written as

$$U = U_{Pm} + U_B \tag{11}$$

Based on the Rayleigh–Ritz method, the displacement functions can be expressed in the following nondimensional form:

J. Eng. Mech. 2007.133:874-886.

$$W(\xi,\eta)=\sum_{i=1}^{I}\sum_{j=1}^{J}C_{ij}^{(1)}\phi_i^{(1)}(\xi)\varphi_j^{(1)}(\eta),\Theta_x^{(k)}(\xi,\eta)$$
$$=\sum_{m=1}^{M}\sum_{n=1}^{N}C_{mn}^{(2k)}\phi_m^{(2k)(\xi)\varphi_n^{(2k)}(\eta)}$$
$$\Theta_y^{(k)}(\xi,\eta)=\sum_{p=1}^{P}\sum_{q=1}^{Q}C_{pq}^{(2k+1)}\phi_p^{(2k+1)}(\xi)\varphi_q^{(2k+1)}(\eta),\quad (k=1-3) \tag{12}$$

where C_{pq}=undetermined displacement coefficient; $\phi(\xi)$, $\varphi(\eta)$=characteristic functions; ξ,η=normalized coordinates; and the superscripts denote displacement coefficients for different layer groups. Herein, the Legendre's orthogonal polynomials are used in Eq. (12) to denote ϕ_i and φ_j. For instance, $\phi_i(\xi)$ is written as

$$\phi_1(\xi)=1$$

$$\phi_2(\xi)=\xi$$

and for $n\geq 3$,

$$\phi_n(\xi)=[(2n-3)\xi\times\phi_{n-1}(\xi)-(n-2)\times\phi_{n-2}(\xi)]/(n-1) \tag{13}$$

where $\xi=(2x/a)-1$ with $-1\leq\xi\leq 1$, and $\eta=(2y/b)-1$ with $-1\leq\eta\leq 1$. It is noted that the above orthogonal polynomials $\phi_i(\xi)$ satisfy the orthogonality condition

$$\int_{-1}^{1}\phi_n(\xi)\phi_m(\xi)d\xi=\begin{cases}0 & \text{if } n\neq m\\ 2/2n-1 & \text{if } n=m\end{cases} \tag{14}$$

Extremization of the functional Π, which is defined as $\Pi=U-T_m$ with respect to the displacement coefficients C_{pq} leads to the following eigenvalue problem

$$[(\mathbf{K})-\omega^2(\mathbf{M})]\{\mathbf{C}\}=0 \tag{15}$$

where $\{\mathbf{C}\}$=vector containing all the displacement coefficients; $(\mathbf{M})$ and $(\mathbf{K})$=structural mass and stiffness matrices of the sandwich plates with elastically restrained edges, respectively. Detailed description of the terms in $(\mathbf{M})$ and $(\mathbf{K})$ are given in the Appendix . If the edge spring constant intensities equal zero, the sandwich plate will have free boundary conditions. The natural frequencies of free laminated composite sandwich plates can be determined from the above equation provided that the material constants of the plates are available. If the actual material constants of the sandwich plate are unknown, trial material constants can be used to predict the theoretical natural frequencies of the plate, which will then be used in the material constant identification method as will be described in the following section to determine the actual material constants of the sandwich plates.

Material Constants Identification

Herein, the aforementioned Rayleigh–Ritz method is applied to the nondestructive evaluation of the elastic constants of laminated composite sandwich plates. The material constant identification of laminated composite sandwich plates using the theoretically predicted and experimentally measured natural frequencies of the plates is formulated as a minimization problem. In mathematical form it is stated as

$$\text{Minimize}\quad e(\mathbf{x})=(\boldsymbol{\omega}^*)^t(\boldsymbol{\omega}^*)$$
$$\text{Subject to}\quad x_i^L\leq x_i\leq x_i^U,\quad (i=1\text{–}6) \tag{16}$$

where $\mathbf{x}=[E_1,E_2,G_{12},\nu_{12},E_c,\nu_c]$=vector containing the design variables which presently are material constants of the composite sandwich plate; $\boldsymbol{\omega}^*=n\times 1$ vector containing the differences between the measured and predicted values of the natural frequencies; $e(\mathbf{x})$=frequency discrepancy function measuring the sum of the squared differences between the predicted and measured data; and x_i^L, x_i^U=lower and upper bounds of the material constants. The elements in $\boldsymbol{\omega}^*$ are expressed as

$$\omega_i^*=\frac{\omega_{pi}-\omega_{mi}}{\omega_{mi}},\quad (i=1-\text{NF}) \tag{17}$$

where ω_{pi}, ω_{mi}=predicted and measured values of the natural frequencies, respectively; and NF=number of natural frequencies. In general, the use of any conventional minimization technique to solve the identification problem of Eq. (16) may encounter great difficulty in obtaining the global minimum, i.e., the actual material constants. For instance, it has been shown that the use of the optimization algorithms of IMSL (1991) to solve Eq. (16) may have a significant converge problem or produce erroneous results that are found unacceptable. Herein, a multistart global minimization method together with an appropriate normalization technique for normalizing the design variables is adopted to solve the above system identification problem. In the proposed method, the above problem of Eq. (16) is first converted into an unconstrained minimization problem by creating the following general augmented Lagrangian as reported in the literature (Vanderplaats 1984)

$$\bar{\boldsymbol{\Psi}}(\tilde{\mathbf{x}},\boldsymbol{\mu},\boldsymbol{\eta},r_p)=e(\tilde{\mathbf{x}})+\sum_{j=1}^{7}[\mu_j z_j+r_p z_j^2+\eta_j\phi_j+r_p\phi_j^2] \tag{18}$$

with

$$z_j=\max\left[g_j(\tilde{x}_j),\quad \frac{-\mu_j}{2r_p}\right],\quad g_j(\tilde{x}_j)=\tilde{x}_j-\tilde{x}_j^{\text{U}}\leq 0$$
$$\phi_j=\max\left[H_j(\tilde{x}_j),\quad \frac{-\eta_j}{2r_p}\right],\quad H_j(\tilde{x}_j)=\tilde{x}_j^L-\tilde{x}_j\leq 0,\quad (j=1-7) \tag{19}$$

where μ_j,η_j,γ_p=multipliers; $\max[*,*]$ takes on the maximum value of the numbers in the bracket. The modified design variables $\tilde{\mathbf{x}}$ are defined as

$$\tilde{\mathbf{x}}=\left[\frac{E_1}{\alpha_1},\frac{E_2}{\alpha_2},\frac{G_{12}}{\alpha_3},\frac{\nu_{12}}{\alpha_4},\frac{E_c}{\alpha_5},\frac{\nu_c}{\alpha_6}\right] \tag{20}$$

where α_i=normalization factor. It is noted that the choice of proper values of the normalization factors can produce appropriate search directions during the minimization process and thus help expedite the convergence of the solution. A detailed study has shown that the suitable values of $\tilde{x}_i(i=1,\ldots,6)$ are better greater than 0 and less than 10. Furthermore, it is worth pointing out that the original design variables are used in the Rayleigh–Ritz method to compute the theoretical natural frequencies for determining the frequency discrepancy function in Eq. (18). The updated formulas for the multipliers μ_j,η_j, and γ_p are

J. Eng. Mech. 2007.133:874-886.

$$\mu_j^{n+1} = \mu_j^n + 2r_p^n Z_j^n, \quad \eta_j^{n+1} = \eta_j^n + 2r_p^n \phi_j^n, \quad (j = 1-7)$$
$$r_p^{n+1} = \begin{cases} \gamma_0 r_p^n & \text{if } r_p^{n+1} < r_p^{\max} \\ r_p^{\max} & \text{if } r_p^{n+1} \geq r_p^{\max} \end{cases} \tag{21}$$

where the superscript n denotes the iteration number; γ_0=constant; and $r_p^{\max}$=maximum value of r_p. Following the guideline given in the literature (Vanderplaats 1984), the parameters μ_j^0, η_j^0, r_p^0, γ_0, $r_p^{\max}$ are chosen as

$$\mu_j^0 = 1.0, \quad \eta_j^0 = 1.0, \quad r_p^0 = 0.4, \quad \gamma_0 = 2.5, \quad r_p^{\max} = 100 \tag{22}$$

The constrained minimization problem of Eq. (16) has thus become the solution of the following unconstrained optimization problem:

$$\text{Minimize} \quad \bar{\Psi}(\tilde{\mathbf{x}}, \boldsymbol{\mu}, \boldsymbol{\eta}, r_p) \tag{23}$$

The above unconstrained optimization problem is to be solved using the previously proposed multistart global optimization algorithm (Snyman and Fatti 1987), which has proven to be able to locate the global minima of unconstrained minimization problems consisting of multiple local minima. In the adopted optimization algorithm, the objective function is treated as the potential energy of a traveling particle and the search trajectories for locating the global minimum are derived from the equation of motion of the particle in a conservative force field. The design variables, i.e., the material constants that make the potential energy of the particle, i.e., objective function, the global minimum constitute the solution of the problem. In the minimization process, a series of starting points for the design variables of Eq. (20) are selected at random from the region of interest. The lowest local minimum along the search trajectory initiated from each starting point is determined and recorded. A Bayesian argument is then used to establish the probability of the current overall minimum value of the objective function being the global minimum, given the number of starts and the number of times this value has been achieved. The multistart optimization procedure is terminated when a target probability, typically, 0.99, has been exceeded.

Experimental Investigation

In the experimental study, a number of laminated composite sandwich plates with different cores and face sheets were fabricated and subjected to impulse vibration testing. The dimensions ($a \times b \times h$) of the laminated composite sandwich plates were 30 cm × 30 cm × 0.375 cm with core thickness of 0.3 cm [Core (I)] or 21 cm × 21 cm × 0.28 cm with core thickness of 0.205 cm [Core (II)]. The face sheets were fabricated using T300/2500 graphite/epoxy (Gr/ep) prepreg tapes produced by Torayca Co., Japan. The cores were made of foam [Core (I)] or plastics [Core (II)] materials. The elastic constants of the Gr/ep face sheets and cores were first determined experimentally using the standard specimens in accordance with ASTM Standards D 3039 and D 695 (ASTM 1990). In the material testing, each elastic constant was determined using three specimens. The means and coefficients of variation (COVs) of the elastic constants obtained from the tests are as follows.

Gr/ep face sheet

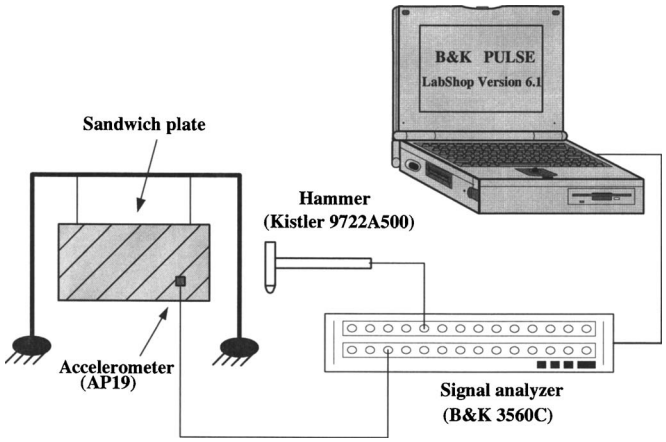

Fig. 3. Impulsive vibration testing of composite sandwich plate

$$E_1 = 146.503 \text{ GPa } (0.72\,\%),$$
$$E_2 = 9.223 \text{ GPa } (1.19\,\%),$$
$$G_{12} = 6.836 \text{ GPa } (3.16\,\%),$$
$$\nu_{12} = 0.306\ (0.19\,\%),$$
$$h_f = 0.375 \text{ mm} \tag{24a}$$

Core

Core (I): $E_c = 27.65$ MPa (3.62 %), $\nu_c = 0.3(0.45\,\%)$, $h_c = 3$ mm

Core (II): $E_c = 3.94$ GPa (2.58 %), $\nu_c = 0.38(0.31\,\%)$,
$$h_c = 2.05 \text{ mm} \tag{24b}$$

The values in the parentheses in the above equation denote the COVs of the elastic constants of the materials. The average mass densities of the core and face sheet of the 30 × 30 cm sandwich plates were 49.1 and 1675.4 Kg/m^3, respectively, while those of the 21 × 21 cm sandwich plates were 1244.1 and 1658.4 Kg/m^3, respectively.

The laminated composite sandwich plate hung by rubber bands was subjected to the impulsive vibration testing as shown in Fig. 3. In the vibration testing of the composite sandwich plate, a hand held impulse hammer (Kistler 9722A500, Kistler Instrument, Amherst, N.Y.) was used to excite the composite sandwich plate at different points on the plate, a force transducer (Kistler 9904A, Kistler Instrument, Amherst, N.Y.) attached to the hammer's head to measure the input force, an accelerometer of mass 0.14 g (AP19, APTechnology, Oosterhout, The Netherlands) to pick up the vibration response data at different locations on the plate, and a data acquisition and analysis system (B&K 3560C and B&K Pulse Labshop Version 6.1) to process the vibration data from which the natural frequencies of the sandwich plates were extracted. It is noted that for each pair of excitation and signal pick-up points, the sandwich plate was tested for several times. Each time when the plate was tested a set of vibration data was produced for constructing the frequency response spectrum of the plate from which the lower natural frequencies of the plates were extracted. A detailed study had shown that the small modal damping ratios with values less than 2% had negligible effects on the lower natural frequencies of the plates and the identified material constants. Therefore, without affecting the generality of the

J. Eng. Mech. 2007.133:874-886.

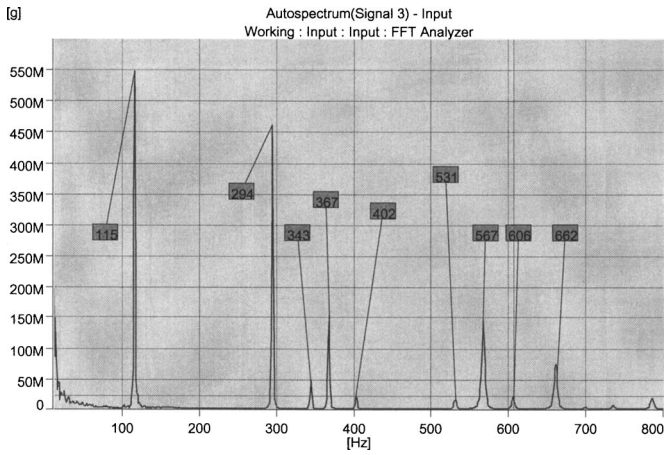

Fig. 4. Frequency response spectrum of the square $[0^0/90^0/0^0/\text{core(I)}/0^0/90^0/0^0]$ plate with free edges

present identification method, when determining the natural frequencies from the frequency response spectra, the frequencies associated with the peak responses were treated as the natural frequencies of the plates. For illustration purposes, Fig. 4 shows a typical frequency response spectrum of the square (30×30 cm) $[0^0_3/\text{core(I)}/0^0_3]$ plate. It is noted that the first six natural frequencies of the plate can be easily identified from the frequency response spectrum as shown in Fig. 4. The means of the first six measured natural frequencies of the free laminated composite sandwich plates determined from the impulsive vibration testing of the plates are listed in Table 1. It is noted that the COVs of the natural frequencies obtained from the tests were less than 0.89%. For comparison purpose, the theoretical natural frequencies of the laminated composite sandwich plates determined using the experimental material constants of Eq. (24*b*) in the present Rayleigh–Ritz method are also listed in Table 1. It is noted that the percentage differences between the experimental and theoretical natural frequencies of the sandwich plates were less than or equal to 8.12%. In the following system identification study, the measured natural frequencies of the sandwich plates in Table 1 will be used in solving the problem of Eq. (16) to demonstrate the applications of the proposed method.

Results and Discussions

A number of numerical examples are first given to illustrate the capability and accuracy of the proposed Raleigh–Ritz method in determining natural frequencies of laminated composite sandwich plates with different boundary conditions reported in the literature or obtained via the use of the finite-element code ANSYS (1997). A convergence study has shown that the uses of $I=J=M=N=P=Q=10$ for the characteristic functions in Eq. (12) are sufficient to make the solutions of the sandwich plates to converge. Therefore, from now on the aforementioned number of terms of the characteristic functions will be used in the Rayleigh–Ritz method for the following sandwich plate analyses. The results obtained by the present method for several free or clamped rectangular laminated composite sandwich plates with different face sheets are listed in Table 2 in comparison with those available in the literature or obtained in the finite-element analyses of the plates using the element type SHELL 91 of ANSYS. It is noted that in analyzing the sandwich plates with simply supported edges, the normalized translational and rotational spring constant intensities are set as 10^{10} and 0, respectively, while those for the plates with clamped edges are set as 10^{10} and 10^6, respectively. It is noted that when comparing with the finite-element results obtained by Watanabe et al. (1993), the natural frequencies of the clamped sandwich plates predicted by the present method are more accurate than those predicted by the previously proposed Rayleigh–Ritz method (Masoud and Pierre 1999) in which the plate deflection and transverse shear forces were represented by an independent set of functions and the rotary inertia effects were neglected. For the free sandwich plates, the natural frequencies produced by the present method closely match those produced by ANSYS. Next consider the effects of edge spring stiffness on the natural frequencies of flexibly supported laminated composite sandwich plates. The material constants of the laminated composite face sheets and core are given as follows:

Table 1. Experimental and Theoretical Natural Frequencies of Free Gr/ep Sandwich Plates

	Natural frequency (Hz)					
Layup	First	Second	Third	Fourth	Fifth	Sixth
$[0^\circ/90^\circ/0^\circ/\text{core(I)}/0^\circ/90^\circ/0^\circ]$	115[a]	294	343	367	402	531
	116.05[b]	297.85	348.24	359.88	395.80	534.10
	−0.90%[c]	−1.29%	−1.51%	1.98%	1.57%	−0.58%
$[0^\circ_3/\text{core(I)}/0^\circ_3]$	118	144	250	331	394	424
	115.55	143.50	251.86	360.25	394.67	423.97
	2.12%	0.35%	−0.74%	−8.12%	−0.17%	0.01%
$[0^\circ/90^\circ/0^\circ/\text{core(II)}/0^\circ/90^\circ/0^\circ]$	120.7	332.7	410.7	447.7	506.3	738
	128.10	335.70	422.96	451.40	517.92	764.83
	−5.77%	−0.89%	−2.90%	−0.82%	−2.24%	−3.51%
$[0^\circ_3/\text{core(II)}/0^\circ_3]$	116	150	279	414.3	529.3	542
	121.29	148.39	287.71	408.08	522.18	548.04
	−4.36%	1.09%	−3.03%	1.52%	1.36%	−1.10%

[a]Experimental natural frequency.

[b]Theoretical natural frequency.

[c]Percentage difference.

J. Eng. Mech. 2007.133:874-886.

Table 2. Natural Frequencies of Rectangular Laminated Composite Sandwich Plates with Different Boundary Conditions

Material	Layup	h_c (mm)	Edge support	Method	Natural frequency (Hz) First	Second	Third
I	$[30_3^0/\overline{\text{core}}]_S$	10	Clamped	Present	709	1,163	1,448
				Masoud and Pierre (1999)	778	1,293	1,599
				Watanabe et al. (1993)	732	1,197	1,477
	$[0_3^0/\overline{\text{core}}]_S$			Present	733	1,268	1,405
				Masoud and Pierre (1999)	752	1,312	1,527
				Watanabe et al. (1993)	716	1,240	1,414
	$[0^0/90^0/0^0/\overline{\text{core}}]_S$	7		Present	694	1,110	1,384
				Masoud and Pierre (1999)	716	1,167	1,497
				Watanabe et al. (1993)	693	1,119	1,412
II	$[0_4^\circ/\text{core}/0_4^\circ]$	3	Free	Present	125.43	166.41	292.61
				ANSYS (1997)	124.75	166.15	290.10
	$[30_4^\circ/\text{core}/30_4^\circ]$			Present	132.23	182.83	290.96
				ANSYS (1997)	131.59	182.32	288.64

Note: Material I: $a=0.45$ m; $b=0.3$ m; $h_f=0.375$ mm; $E_1=105$ GPa; $E_2=8.74$ GPa; $G_{12}=4.56$ GPa; $\nu_{12}=0.327$; $\rho_f=1{,}600$ kg/m^3; $G_{xz}=103$ MPa; $G_{yz}=62.1$ MPa; and $\rho_c=16$ kg/m^3.

Material II: $a=0.3$ mm; $b=0.3$ mm; $h_f=0.5$ mm; $E_1=150$ GPa; $E_2=10$ GPa; $G_{12}=6$ GPa; $G_{23}=2$ GPa; $\nu_{12}=0.3$; $\rho_f=1550$ kg/m^3; $E_c=100$ MPa; $G_c=38.46$ Mpa; and $\rho_c=50$ kg/m^3.

$$\text{Face sheets: } E_1/E_2=15,\quad G_{12}/E_2=0.6,\quad G_{23}/E_2=0.1,$$
$$\nu_{12}=0.3,\quad E_2=10\text{ Gpa},\quad \rho_f=1500\text{ kg/m}^3$$

$$\text{Core: } E_c=10\text{ MPa}\quad\text{or}\quad 1\text{ GPa},\quad G_c=E_c/(2+2\nu_c),$$
$$\nu_c=0.3,\quad \rho_c=50\text{ kg/m}^3$$

$$b=0.3\text{ m},\quad h_f=0.5\text{ mm},\quad h_c=9\text{ mm} \tag{25}$$

The first five natural frequencies of the $[(0^\circ/90^\circ)_S/\overline{\text{core}}]_S$ and $[(45^\circ/-45^\circ)_S/\overline{\text{core}}]_S$ plates supported by edge springs with different spring constant intensities are listed in Tables 3 and 4, respectively. It is noted that the stiffness of translational springs, core property, lamination arrangement of face sheets, and aspect ratio have more effects on the natural frequencies of the sandwich plates than the stiffness of rotational springs. For instance, consider different cases of the $[(0^\circ/90^\circ)_S/\overline{\text{core}}]_S$ plate with $E_c=10$ MPa in Table 3. For the plate with the normalized translational spring constant intensity $K=1$ and aspect ratio $a/b=0.5$, the first normalized natural frequency merely increases 0.21% from 14.19 to 14.22 when the normalized rotational spring constant intensity R increases from 1 to 10^6. For the plate with $K=R=1$, the first normalized natural frequency has a significant reduction of 72.87% from 14.19 to 3.85 as the aspect ratio changes from 0.5 to 2. For the plate with $a/b=0.5$ and $R=1$, the first normalized natural frequency increases 93.8% from 14.19 to 27.5 as K increases from 1 to 10^{10}. The core rigidity also has significant effects on the natural frequencies of the plate. For instance, for the plate with $K=10^{10}$, $R=10^6$, and $a/b=0.5$, the first normalized natural frequency increases 526.18% from 27.81 to 174.14 as E_c changes from 10 MPa to 1 GPa. Furthermore, such effects will become more prominent when the mode number increases. For instance, for the same case, comparing to the 526.18% increase for the first mode, there is a 585.6% increase for the fifth mode. Comparing the results in Table 3 with those in Table 4, it is also noted that fiber angles of face sheets can affect the natural frequencies of the sandwich plates. For instance, the first normalized natural frequency of the $[(0^\circ/90^\circ)_S/\overline{\text{core}}]_S$ plate is 150.05% higher than that of the $[(45^\circ/-45^\circ)_S/\overline{\text{core}}]_S$ plate when $K=10$, $R=1$, $a/b=0.5$, and $E_c=10$ MPa.

Now a theoretical study of the capability and accuracy of the present method in identifying material constants of laminated composite sandwich plates is first given. The first six theoretical natural frequencies of the flexibly supported $[0^0/90^0/0^0/\text{core(I)}/0^0/90^0/0^0]$ plate in Table 1 are treated as "measured" natural frequencies in the identification of the material constants of the sandwich plate. The upper and lower bounds of the material constants chosen based on experience are reasonably large

$$0\le E_1\le 400\text{ GPa};\quad 0\le E_2\le 40\text{ GPa};\quad 0\le G_{12}\le 20\text{ GPa}$$

$$0\le \nu_{12}\le 0.5;\quad 0\le E_c\le 100\text{ MPa};\quad 0\le \nu_c\le 0.5 \tag{26}$$

The modified design variables of Eq. (20) when obtained via the use of the following normalization factors are less than 10:

$$\alpha_1=\alpha_5=100,\quad \alpha_4=\alpha_6=1$$

and

$$\alpha_i=10\quad (i=2,3) \tag{27}$$

Since the modified design variables are less than 10, the search for the solution can thus be expedited. In the identification process, four starting points are randomly generated and for each starting point around 18 iterations are required to locate the lowest local minimum. The starting points, the lowest local minima for the starting points, numbers of iterations required to obtain the lowest local minima, and the global minimum are listed in Table 5. It is noted that the actual material constants have been identified in an efficient and effective way. Next, consider the system identification of free square (21 cm × 21 cm) $[0_3^\circ/\text{core}/0_3^\circ]$ and $[45^\circ/-45^\circ/45^\circ/\text{core}/45^\circ/-45^\circ/45^\circ]$ plates with faces made of Gr/ep or glass/epoxy (Gl/ep) materials. The actual properties of the Gr/ep and Gl/ep sandwich plates are as follows:

J. Eng. Mech. 2007.133:874-886.

Table 3. Normalized Natural Frequencies of Flexibly Supported $[(0°/90°)_S/\overline{\text{core}}]_S$ Plates with Different Aspect Ratios and Core Materials

				Normalized natural frequency λ[a]				
E_c	K	R	a/b	First	Second	Third	Fourth	Fifth
10 MPa	1	1	0.5	14.19	17.07	25.82	29.77	31.83
			1	5.28	10.82	10.86	15.3	22.19
			2	3.85	4.93	10.2	10.28	11.26
		10^6	0.5	14.22	17.87	26.22	30.51	32.49
			1	5.3	12.13	12.19	16.56	22.66
			2	3.86	5.88	11.01	11.59	12.51
	10	1	0.5	24.48	28.59	35.36	43.4	48.16
			1	12.02	18.95	19.14	24.35	28.12
			2	8.81	10.02	13.57	17.06	17.94
		10^6	0.5	24.69	28.81	35.59	43.81	48.31
			1	12.24	19.21	19.55	24.59	28.31
			2	9	10.56	14.07	17.35	18.25
	10^{10}	1	0.5	27.5	33.84	42.68	52.68	54.59
			1	15.66	25.14	25.92	32.58	36.12
			2	11.92	15.32	20.06	22.99	24.94
		10^6	0.5	27.81	34.08	42.78	52.8	54.74
			1	16.16	25.28	26.12	32.6	36.23
			2	12.47	15.64	20.31	23.1	25.01
1 GPa	1	1	0.5	16.05	22.33	58.54	68.48	72.47
			1	5.52	16.47	16.52	28.18	70.5
			2	4.02	5.89	16.02	18.62	19.62
		10^6	0.5	16.12	31.26	98.7	99.93	107.76
			1	5.53	27.3	27.36	41.77	97.53
			2	4.03	8.02	26.83	27.08	29.22
	10	1	0.5	47.69	52.57	87.55	95.58	102.77
			1	16.63	27.47	27.5	38.68	74.56
			2	12.12	13.44	23.27	24.94	26.89
		10^6	0.5	49.45	57.45	109.85	119.94	127.05
			1	17.2	33.96	34	47.85	99.61
			2	12.54	14.63	29.5	31.84	33.81
	10^{10}	1	0.5	122.43	162.3	240.53	323.65	341.12
			1	49.4	112.78	112.9	155.87	207.5
			2	35.28	46.83	72.31	105.47	109.37
		10^6	0.5	174.14	213.37	284.02	358.4	375.3
			1	77.85	144.05	144.16	190.98	234.97
			2	56.64	68.79	93.97	130.28	132.55

[a]$\lambda=\omega b^2\sqrt{\rho_f H/D_{11}}$; $H=2h_f+h_c$; and D_{11}=bending stiffness in the x direction. $K=K_{L1}\times a^3/D_{11}=K_{L2}\times a^3/D_{11}=K_{L3}\times b^3/D_{22}=K_{L4}\times b^3/D_{22}$; $R=R_{L1}\times a/D_{11}=R_{L2}\times a/D_{11}=R_{L3}\times b/D_{22}=R_{L4}\times b/D_{22}$.

Gr/ep sandwich plate

$$E_1=131\text{ GPa},\quad E_2=11.2\text{ GPa},\quad G_{12}=6.55\text{ GPa},\quad \nu_{12}=0.28 \tag{28a}$$

$$\rho_f=1{,}550\text{ kg/m}^3,\quad h_f=0.375\text{ mm},\quad \rho_c=500\text{ kg/m}^3,\quad h_c=2\text{ mm}$$

Gl/ep sandwich plate

$$E_1=38.6\text{ GPa},\quad E_2=8.27\text{ GPa},\quad G_{12}=4.14\text{ GPa},\quad \nu_{12}=0.26$$

$$\rho_f=1{,}800\text{ kg/m}^3,\quad h_f=0.375\text{ mm},\quad \rho_c=500\text{ kg/m}^3,\quad h_c=2\text{ mm} \tag{28b}$$

The actual natural frequencies of the Gr/ep and Gl/ep sandwich plates with different core properties are listed in Table 6. Again, the first six actual natural frequencies, which are treated as the "measured" natural frequencies, are used in the present method to identify the material constants of the Gl/ep sandwich plates. The bounds of the material constants chosen to be reasonably large are as the following:

$$0\le E_1\le 400\text{ GPa};\quad 0\le E_2\le 40\text{ GPa};\quad 0\le G_{12}\le 20\text{ GPa};\quad 0\le \nu_{12}\le 0.5$$

$$0\le E_c\le 100\text{ MPa};\quad 0\le \nu_c\le 0.5\quad \text{for } E_c=10\text{ MPa}$$

Table 4. Normalized Natural Frequencies of Flexibly Supported $[(45°/-45°)_S/\overline{\text{core}}]_S$ Plates with Different Aspect Ratios and Core Materials

				Normalized natural frequency λ[a]				
E_c	K	R	a/b	First	Second	Third	Fourth	Fifth
10 MPa	1	1	0.5	4.25	7.35	9.91	13.66	17.79
			1	2.28	3.73	6.38	8.61	9.09
			2	13.52	15.77	22.99	28.62	30.16
		10^6	0.5	4.26	9.01	10.95	14.4	18.94
			1	2.29	4.67	8.2	9.61	9.92
			2	21.84	24	29.23	36.51	44.17
	10	1	0.5	9.79	13.7	17.18	20.33	21.64
			1	6.04	7.59	11.14	11.28	12.86
			2	22.03	24.29	29.86	37.26	44.29
		10^6	0.5	9.99	14.29	17.4	20.65	22.22
			1	6.23	8	11.68	11.79	13.33
			2	24.57	30.02	37.86	46.68	49.38
	10^{10}	1	0.5	13.61	21.77	23.23	28.91	31.6
			1	9.95	13.35	17.8	19.63	21.71
			2	24.97	30.11	38.06	46.83	49.5
		10^6	0.5	14.24	22.04	23.45	29.13	31.82
			1	10.75	13.82	18.12	19.89	21.98
			2	4.25	7.35	9.91	13.66	17.79
1 GPa	1	1	0.5	15.72	17.9	40.14	57.35	75.19
			1	4.47	9.66	15.86	27.63	41.47
			2	2.38	4.83	9.05	14.93	18.95
		10^6	0.5	15.78	20.85	54.79	95.78	107.67
			1	4.48	14.51	26.46	38.84	54.59
			2	2.39	7.09	14.36	20.28	26.07
	10	1	0.5	46.42	48.29	61.66	94.01	96.99
			1	13.46	18.16	25.47	34.17	45.25
			2	7.19	9.23	14.13	18.47	21.02
		10^6	0.5	48.15	50.56	71.61	116.11	120.2
			1	13.91	20.71	31.87	42.98	56.75
			2	7.44	10.44	17.36	22.58	27.23
	10^{10}	1	0.5	119.18	145.44	190.75	252.28	306.61
			1	44.34	79.74	111.89	127.85	150.35
			2	24.12	40.63	66.43	66.69	81.7
		10^6	0.5	159.11	181.32	222.14	279.95	331.72
			1	64.37	101.08	135.07	150.4	173.39
			2	36.13	53.83	81.22	84.21	99.27

[a]$\lambda=\omega b^2\sqrt{\rho_f H/D_{11}}$; $H=2h_f+h_c$; and D_{11} is bending stiffness in the x direction. $K=K_{L1}\times a^3/D_{11}=K_{L2}\times a^3/D_{11}=K_{L3}\times b^3/D_{22}=K_{L4}\times b^3/D_{22}$; $R=R_{L1}\times a/D_{11}=R_{L2}\times a/D_{11}=R_{L3}\times b/D_{22}=R_{L4}\times b/D_{22}$.

J. Eng. Mech. 2007.133:874-886.

Table 5. Identified Elastic Constants of the Gr/ep $[0^0/90^0/0^0/\text{core(I)}/0^0/90^0/0^0]$ Sandwich Plate with Free Edges Using Actual Natural Frequencies

		System parameter						
Starting point number	Stage	E_1 (GPa)	E_2 (GPa)	G_{12} (GPa)	ν_{12}	E_c (MPa)	ν_c	Number of iterations
1	Initial	286.5625	37.4817	12.5915	0.1994	24.1326	0.4875	17
	Final	146.5030	9.2230	6.8360	0.3060	27.6500	0.3000	
2	Initial	96.1479	21.0436	19.8511	0.4634	78.2327	0.3255	16
	Final	146.5030	9.2230	6.8360	0.3060	27.6500	0.3000	
3	Initial	197.2084	10.8297	7.7575	0.1176	79.4014	0.4949	18
	Final	146.5030	9.2230	6.8360	0.3060	27.6500	0.3000	
4	Initial	75.4331	0.4824	13.7528	0.1648	36.9631	0.2519	21
	Final	146.5030	9.2230	6.8360	0.3060	27.6500	0.3000	
Global minimum		146.5030	9.2230	6.8360	0.3060	27.65	0.3000	Probability
	(0%)	(0%)	(0%)	(0%)	(0%)	(0%)	(0%)	0.9921

Values in parentheses denote percentage difference between identified and actual data.

Table 6. Actual Natural Frequencies of Free Gr/ep and Gl/ep Sandwich Plates

			Natural frequency (Hz)					
Material	Layup	Core E_c (Mpa)	First	Second	Third	Fourth	Fifth	Sixth
Gr/ep	$[0^\circ_3/\text{core}/0^\circ_3]$	10	114.1928	162.6302	234.8167	290.6084	314.7152	341.8780
		2,000	149.0150	200.6343	362.4224	550.6015	617.0932	684.6992
	$[45^\circ/-45^\circ/45^\circ/\text{core}/45^\circ/-45^\circ/45^\circ]$	10	174.2297	183.6306	252.9345	287.4444	297.7229	406.9070
		2,000	247.7889	317.7901	468.3839	694.9438	715.9061	1,005.9287
Gl/ep	$[0^\circ_3/\text{core}/0^\circ_3]$	10	96.5056	145.0586	209.7339	234.8041	264.8337	316.9234
		2,000	124.8429	176.6204	308.3220	361.4576	434.5461	491.9069
	$[45^\circ/-45^\circ/45^\circ/\text{core}/45^\circ/-45^\circ/45^\circ]$	10	131.1276	153.3775	200.8882	244.4192	254.4609	358.5897
		2,000	183.4542	186.9897	278.6001	417.4645	445.1689	647.3830

Table 7. System Identification of Gr/ep and Gl/ep Sandwich Plates Using Actual Natural Frequencies

					System parameter					
Material	Layup	Core E_c (MPa)	Number of starting points	Average number of iteration	E_1 (GPa)	E_2 (GPa)	G_{12} (GPa)	ν_{12}	E_c (MPa)	ν_c
Gr/ep	$[0^\circ_3/\text{core}/0^\circ_3]$	10	6	21	131.0 (0%)	11.2 (0%)	6.55 (0%)	0.28 (0%)	10.0285 (0.29%)	0.3017 (0.57%)
		2,000	6	20	131.0 (0%)	11.2 (0%)	6.55 (0%)	0.28 (0%)	2000 (0%)	0.3 (0%)
	$[45^\circ/-45^\circ/45^\circ/\text{core } 45^\circ/-45^\circ/45^\circ]$	10	4	19	131.0 (0%)	11.1998 (1.79e-3%)	6.55 (0%)	0.28 (0%)	10.0585 (0.29%)	0.3017 (0.73%)
		2,000	7	24	130.998 (−1.53e-3%)	11.1973 (−0.024%)	6.5500 (0%)	0.2798 (0.07%)	2002.28 (0.114%)	0.3015 (0.5%)
Gl/ep	$[0^\circ_3/\text{core}/0^\circ_3]$	10	7	15	38.6 (0%)	8.27 (0%)	4.14 (0%)	0.26 (0%)	10.01 (0.1%)	0.3014 (0.47%)
		2,000	6	14	38.6 (0%)	8.27 (0%)	4.14 (0%)	0.26 (0%)	2000 (0%)	0.3 (0%)
	$[45^\circ/-45^\circ/45^\circ/\text{core } 45^\circ/-45^\circ/45^\circ]$	10	6	17	38.6 (0%)	8.27 (0%)	4.14 (0%)	0.26 (0%)	10 (0%)	0.3001 (0.03%)
		2,000	10	14	38.6 (0%)	8.27 (0%)	4.14 (0%)	0.26 (0%)	2000 (0%)	0.3 (0%)

Note: Values in the parentheses denote percentage difference between identified and actual data.

J. Eng. Mech. 2007.133:874-886.

Table 8. Identified Material Constants of the Gr/ep $[0^0/90^0/0^0/\text{core(I)}/0^0/90^0/0^0]$ Sandwich Plate Using Experimental Natural Frequencies

Starting point number	Stage	System parameter E_1 (GPa)	E_2 (GPa)	G_{12} (GPa)	ν_{12}	E_c (MPa)	ν_c	Number of iterations
1	Initial	167.897	4.942	2.081	0.400	1.318	0.304	14
	Final	140.946	8.514	6.517	0.300	29.821	0.300	
2	Initial	45.092	6.529	7.893	0.266	17.779	0.126	11
	Final	140.947	8.514	6.517	0.300	29.821	0.300	
3	Initial	320.411	14.503	4.623	0.158	93.779	0.243	13
	Final	140.946	8.514	6.517	0.300	29.821	0.300	
4	Initial	172.861	27.980	6.510	0.499	30.321	0.101	12
	Final	140.947	8.514	6.517	0.300	29.821	0.300	
Global minimum		140.946 (−3.79%)	8.514 (−7.69%)	6.517 (−4.67%)	0.300 (−1.96%)	29.821 (7.85%)	0.300 (0%)	Probability 0.9921

Note: Values in the parentheses denote percentage difference between identified and measured data. Measured elastic constants: $E_1=146.503$ GPa; $E_2=9.223$ GPa; $G_{12}=6.836$ GPa; $\nu_{12}=0.306$; and Core(I): $E_c=27.65$ MPa, $\nu_c=0.3$.

$$0 \le E_c \le 10{,}000 \text{ MPa}; \quad 0 \le \nu_c \le 0.5 \quad \text{for } E_c = 2{,}000 \text{ MPa} \tag{29}$$

The modified design variables of the Gl/ep sandwich plates when obtained via the use of the following normalization factors are less than 10:

$$\alpha_1 = 100, \quad \alpha_4 = \alpha_6 = 1, \quad \alpha_i = 10, \quad (i = 2,3)$$

and

$$\alpha_5 = 100 \quad \text{for } E_c = 10 \text{ MPa}$$

$$\alpha_5 = 10{,}000 \quad \text{for } E_c = 2{,}000 \text{ MPa} \tag{30}$$

The numbers of starting points and the average numbers of iterations required to obtain the global minima for the cases are listed in Table 7. Again, for all the cases under consideration, the actual material constants of the sandwich plates can be determined in an efficient and effective way.

Finally, the present method is applied to the identification of material constants of the Gr/ep composite sandwich plates that have been tested. The first six measured natural frequencies of the $[0^0/90^0/0^0/\text{core(I)}/0^0/90^0/0^0]$ sandwich plate in Table 1 are used as an example to illustrate the system identification process of the present method. Table 8 lists the randomly generated starting points, the lowest local minima obtained for the starting points, the numbers of iterations required to get the lowest local minima, and the global minimum. It is noted that very good estimates of the material constants with percentage differences less than or equal to 7.85% have been obtained for the $[0^0/90^0/0^0/\text{core(I)}/0^0/90^0/0^0]$ sandwich plate. For the other sandwich plates, the numbers of starting points, the average numbers of iterations, the identified system parameters, and the percentage differences between the actual and identified system parameters are listed in Table 9. In view of the identified system parameters listed in Table 9, it is noted that the percentage differences between the actual and identified material constants for the sandwich plates are less than or equal to 12.9%. In general, among any set of the identified material constants, only one of the material constants may have relatively large percentage difference while those of the other identified material constants are small. Though for engineering applications, percentage differences of material constants less than 15% have always found to be acceptable, more in-depth investigation should be pursued to improve the accuracy of the identified material constants in the future. Further study has shown that the use of over six natural frequencies in the identification process will produce similar results. Finally, it is worth pointing out that the differences between the identified and actual material constants of the plates that have been tested in this study may be due to a number of uncertain factors (Lauwagie et al. 2006), including, for instance, the effects of accelerometer mass on the plate vibration and existence of noise in the measurement data of tensile and vibration tests. Regarding the effects induced by accelerometer mass, the use of noncontact probes to measure plate vibration responses can eliminate the adverse effects of accelerometer mass imposed on plate vibration. On the other hand, the effects of the measurement noise

Table 9. Identified Material Constants of Different Laminated Composite Sandwich Plates Using Experimental Natural Frequencies

Layup	Number of starting points	Average number of iteration	System parameter E_1 (GPa)	E_2 (GPa)	G_{12} (GPa)	ν_{12}	E_c (MPa)	ν_c
$[0^\circ_3/\text{core(I)}/0^\circ_3]$	4	13	155.075 (5.85%)	8.884 (−3.68%)	6.942 (1.55%)	0.3 (−1.96%)	26.343 (−4.73%)	0.3 (0%)
$[0^\circ/90^\circ/0^\circ/\text{core(II)}/0^\circ/90^\circ/0^\circ]$	6	17	148.571 (1.41%)	9.462 (2.59%)	6.057 (−11.40%)	0.3004 (−1.85%)	3,529.123 (−10.43%)	0.3706 (−2.48%)
$[0^\circ_3/\text{core(II)}/0^\circ_3]$	4	24	145.716 (−0.55%)	8.553 (−7.26%)	5.954 (−12.90%)	0.2920 (−4.58%)	3942.755 (0.07%)	0.3748 (−1.39%)

Notes: Values in the parentheses denote percentage difference between identified and measured data. Measured elastic constants: $E_1=146.503$ GPa; $E_2=9.223$ GPa; $G_{12}=6.836$ GPa; $\nu_{12}=0.306$; Core(I): $E_c=27.65$ MPa; $\nu_c=0.3$; Core(II): $E_c=3.94$ GPa; $\nu_c=0.38$.

J. Eng. Mech. 2007.133:874-886.

on the identified system parameters and the sources of the noise should be studied in detail so that the measurement noise incurred in the vibration testing of the plates can be suppressed or the detrimental effects of the measurement noise be minimized or even eliminated.

Conclusions

A method has been presented for free vibration analysis of laminated composite sandwich plates with different boundary conditions. Several examples have been given to demonstrate the accuracy of the proposed method. The present method has been used in the material constants identification of laminated composite sandwich plates via a vibration testing approach. The identification process has included the extraction of natural frequencies from vibration test data, the utilization of the present method for predicting the theoretical natural frequencies of the laminated composite sandwich plates using trial values of the material constants, the construction of the frequency discrepancy function that measures the sum of the differences between the experimental and theoretical predictions of the system natural frequencies, and the use of a multistart global minimization method to identify the elastic constants by making the frequency discrepancy function the global minimum. Both numerical and experimental investigations have been conducted to demonstrate the capability, effectiveness, accuracy, and applications of the material constant identification procedure. In the theoretical study, it has been shown that the identification procedure can identify the actual material constants of free laminated composite sandwich plates made of different laminated composite materials using the first six natural frequencies in an efficient and effective way. In the experimental investigation, several Gr/ep $[0^0/90^0/0^0/\text{core(I)}/0^0/90^0/0^0]$, $[0_3/\text{core(I)}/0_3^0]$, $[0^0/90^0/0^0/\text{core(II)}/0^0/90^0/0^0]$, and $[0_3/\text{core(II)}/0_3^0]$ sandwich plates with different core materials have been subjected to impulsive vibration testing to measure the lower natural frequencies of the plates. The uses of the first six measured natural frequencies in the identification procedure can also produce estimates of the material constants with acceptable accuracy. The largest percentage difference between the actual and identified material constant obtained in this study is 12.90% for the face-layer in-plane shear modulus G_{12} while small percentage differences have been obtained for the other material constants. The possible factors that may cause error in identifying the material constants and ways for improving the accuracy of the identified material constants have been discussed. The present identification procedure has the potential to be used as a preliminary technique for quick material constant evaluation.

Acknowledgments

This research work was supported by the National Science Council of the Republic of China under Grant No. NSC 94-2212-E-009-020. Its support is gratefully appreciated.

Appendix. Elements of System Matrices *K* and *M* of Symmetrically Laminated Composite Sandwich Plates with Free Edges

The eigenvalue problem of Eq. (15) is rewritten as

$$\left(\begin{bmatrix} K^{11} & K^{12} & K^{13} & K^{14} & K^{15} \\ & K^{22} & K^{23} & K^{24} & K^{25} \\ & & K^{33} & K^{34} & K^{35} \\ \text{symmetric} & & & K^{44} & K^{45} \\ & & & & K^{55} \end{bmatrix} - \omega^2 \begin{bmatrix} M^{11} & 0 & 0 & 0 & 0 \\ & M^{22} & 0 & M^{24} & 0 \\ & & M^{33} & 0 & M^{35} \\ \text{symmetric} & & & M^{44} & 0 \\ & & & & M^{55} \end{bmatrix} \right) \begin{Bmatrix} C_{ij}^{(1)} \\ C_{mn}^{(2)} \\ C_{pq}^{(3)} \\ C_{m'n'}^{(4)} \\ C_{p'q'}^{(5)} \end{Bmatrix} = \begin{Bmatrix} 0 \\ 0 \\ 0 \\ 0 \\ 0 \end{Bmatrix} \tag{31}$$

where

$$[K^{11}]_{ijij}^{--} = 4 \times [(A_{44}^c + 2A_{44}^f)E_{ii}^{00}F_{jj}^{11}/b^2 + (A_{55}^c + 2A_{55}^f)E_{ii}^{11}F_{jj}^{00}/a^2 + (A_{45}^c + 2A_{45}^f)(E_{ii}^{01}F_{jj}^{10} + E_{ii}^{10}F_{jj}^{01})/(ab)] + 2 \times \{F_{jj}^{00}[K_{L1}\phi_i(-1)\phi_{\bar{i}}(-1) + K_{L2}\phi_i(1)\phi_{\bar{i}}(1)]/a + E_{ii}^{00}[K_{L3}\varphi_j(-1)\varphi_{\bar{j}}(-1) + K_{L4}\varphi_j(1)\varphi_{\bar{j}}(1)]/b\}$$

$$[K^{12}]_{ijmn} = 2 \times (A_{45}^c E_{im}^{00}F_{jn}^{10}/b + A_{55}^c E_{im}^{10}F_{jn}^{00}/a)$$

$$[K^{13}]_{ijpq} = 2 \times (A_{44}^c E_{ip}^{00}F_{jq}^{10}/b + A_{45}^c E_{ip}^{10}F_{jq}^{00}/a)$$

$$[K^{14}]_{ijm'n'} = 4 \times (A_{45}^f E_{im'}^{00}F_{jn'}^{10}/b + A_{55}^f E_{im'}^{10}F_{jn'}^{00}/a)$$

$$[K^{15}]_{ijp'q'} = 4 \times (A_{44}^f E_{ip'}^{00}F_{jq'}^{10}/b + A_{45}^f E_{ip'}^{10}F_{jq'}^{00}/a)$$

$$[K^{22}]_{mnm\bar{m}n} = A_{55}^c E_{m\bar{m}}^{00}F_{n\bar{n}}^{00} + (4D_{11}^c + 2A_{11}^f \times h_c^2) \times E_{m\bar{m}}^{11}F_{n\bar{n}}^{00}/a^2 + (4D_{13}^c + 2A_{13}^f \times h_c^2)(E_{m\bar{m}}^{01}F_{n\bar{n}}^{10} + E_{m\bar{m}}^{10}F_{n\bar{n}}^{01})/(ab) + (4D_{33}^c + 2A_{33}^f \times h_c^2) \times E_{m\bar{m}}^{00}F_{n\bar{n}}^{11}/b^2 + 2 \times F_{n\bar{n}}^{00} \times [K_{R1}\phi_m(-1)\phi_{\bar{m}}(-1) + K_{R2}\phi_m(1)\phi_{\bar{m}}(1)]/a$$

$$[K^{23}]_{mnpq} = A_{45}^c E_{mp}^{00}F_{nq}^{00} + (4D_{13}^c + 2A_{13}^f \times h_c^2)E_{mp}^{11}F_{nq}^{00}/a^2 + [(4D_{12}^c + 2A_{12}^f \times h_c^2)E_{mp}^{10}F_{nq}^{01} + (4D_{33}^c + 2A_{33}^f \times h_c^2) \times E_{mp}^{01}F_{nq}^{10}]/(ab) + (4D_{23}^c + 2A_{23}^f \times h_c^2)E_{mp}^{00}F_{nq}^{11}/b^2$$

$$[K^{24}]_{mnm'n'} = 4h_c \times [B_{11}^f E_{mm'}^{11}F_{nn'}^{00}/a^2 + B_{33}^f E_{mm'}^{00}F_{nn'}^{11}/b^2 + B_{13}^f (E_{mm'}^{10}F_{nn'}^{01} + E_{mm'}^{01}F_{nn'}^{10})/(ab)]$$

J. Eng. Mech. 2007.133:874-886.

$$[K^{25}]_{mnp'q'} = 4h_c \times [B^f_{13}E^{11}_{mp'}F^{00}_{nq'}/a^2 + B^f_{23}E^{00}_{mp'}F^{11}_{nq'}/b^2 + (B^f_{12}E^{10}_{mp'}F^{01}_{nq'} + B^f_{33}E^{01}_{mp'}F^{10}_{nq'})/(ab)]$$

$$[K^{33}]_{pq\bar{p}\bar{q}} = A^c_{44}E^{00}_{p\bar{p}}F^{00}_{q\bar{q}} + (4D^c_{33} + 2A^f_{33} \times h_c^2)E^{11}_{p\bar{p}}F^{00}_{q\bar{q}}/a^2 + (4D^c_{22} + 2A^f_{22} \times h_c^2)E^{00}_{p\bar{p}}F^{11}_{q\bar{q}}/b^2 + (4D^c_{23} + 2A^f_{23} \times h_c^2) \times (E^{10}_{p\bar{p}}F^{01}_{q\bar{q}} + E^{01}_{p\bar{p}}F^{10}_{q\bar{q}})/(ab) + 2 \times E^{00}_{p\bar{p}}[K_{R3}\varphi_q(-1)\varphi_{\bar{q}}(-1) + K_{R4}\varphi_q(1)\varphi_{\bar{q}}(1)]/b$$

$$[K^{34}]_{pqm'n'} = 4h_c \times [B^f_{13}E^{11}_{pm'}F^{00}_{qn'}/a^2 + B^f_{23}E^{00}_{pm'}F^{11}_{qn'}/b^2 + (B^f_{33}E^{10}_{pm'}F^{01}_{qn'} + B^f_{12}E^{01}_{pm'}F^{10}_{qn'})/(ab)]$$

$$[K^{35}]_{pqp'q'} = 4h_c \times [B^f_{33}E^{11}_{pp'}F^{00}_{qq'}/a^2 + B^f_{22}E^{00}_{pp'}F^{11}_{qq'}/b^2 + B^f_{23}(E^{10}_{pp'}F^{01}_{qq'} + E^{01}_{pp'}F^{10}_{qq'})/(ab)]$$

$$[K^{44}]_{m'n'\bar{m}'\bar{n}'} = 2 \times \{A^f_{55}E^{00}_{m\bar{m}'}F^{00}_{n\bar{n}'} + 4 \times [D^f_{11}E^{11}_{m\bar{m}'}F^{00}_{n\bar{n}'}/a^2 + D^f_{33}E^{00}_{m\bar{m}'}F^{11}_{n\bar{n}'}/b^2 + D^f_{13}(E^{10}_{m\bar{m}'}F^{01}_{n\bar{n}'} + E^{01}_{m\bar{m}'}F^{10}_{n\bar{n}'})/(ab)] + 2 \times F^{00}_{n'\bar{n}'}[K_{R1}\phi_{m'}(-1)\phi_{\bar{m}'}(-1) + K_{R2}\phi_{m'}(1)\phi_{\bar{m}'}(1)]/a\}$$

$$[K^{45}]_{m'n'p'q'} = 2 \times \{A^f_{45}E^{00}_{m'p'}F^{00}_{n'q'} + 4 \times [D^f_{13}E^{11}_{m'p'}F^{00}_{n'q'}/a^2 + D^f_{23}E^{00}_{m'p'}F^{11}_{n'q'}/b^2 + (D^f_{12}E^{10}_{m'p'}F^{01}_{n'q'} + D^f_{33}E^{01}_{m'p'}F^{10}_{n'q'})/(ab)]\}$$

$$[K^{55}]_{p'q'\bar{p}'\bar{q}'} = 2 \times \{A^f_{44}E^{00}_{p'\bar{p}'}F^{00}_{q'\bar{q}'} + 4 \times [D^f_{33}E^{11}_{p'\bar{p}'}F^{00}_{q'\bar{q}'}/a^2 + D^f_{22}E^{00}_{p'\bar{p}'}F^{11}_{q'\bar{q}'}/b^2 + D^f_{23}(E^{10}_{p'\bar{p}'}F^{01}_{q'\bar{q}'} + E^{01}_{p'\bar{p}'}F^{10}_{q'\bar{q}'})/(ab)] + 2 \times E^{00}_{p\bar{p}'}[K_{R3}\varphi_{q'}(-1)\varphi_{\bar{q}'}(-1) + K_{R4}\varphi_{q'}(1)\varphi_{\bar{q}'}(1)]/b\}$$

$$[M^{11}]_{ij\bar{i}\bar{j}} = (\rho_c h_c + 2\rho_f h_f)E^{00}_{i\bar{i}}F^{00}_{j\bar{j}}$$

$$[M^{22}]_{mn\bar{m}\bar{n}} = (\rho_c h_c^3/12 + \rho_f h_c^2 h_f/2)E^{00}_{m\bar{m}}F^{00}_{n\bar{n}}$$

$$[M^{24}]_{mnm'n'} = 2 \times \rho_f h_c h_f^2 \times E^{00}_{mm'}F^{00}_{nn'}/4$$

$$[M^{33}]_{pq\bar{p}\bar{q}} = (\rho_c h_c^3/12 + \rho_f h_c^2 h_f/2)E^{00}_{p\bar{p}}F^{00}_{q\bar{q}}$$

$$[M^{35}]_{pqp'q'} = 2 \times \rho_f h_c h_f^2 \times E^{00}_{pp'}F^{00}_{qq'}/4$$

$$[M^{44}]_{m'n'\bar{m}'\bar{n}'} = 2 \times \rho_f h_f^3 \times E^{00}_{m'\bar{m}'}F^{00}_{n\bar{n}'}/3$$

$$[M^{55}]_{p'q'\bar{p}'\bar{q}'} = 2 \times \rho_f h_f^3 \times E^{00}_{p'\bar{p}'}F^{00}_{q\bar{q}'}/3$$

$$r,s = 0,1; i,j,\bar{i},\bar{j},i',j',\bar{i}',\bar{j}' = 1,2,3,\cdots I,J;$$
$$m,n,\bar{m},\bar{n},m',n',\bar{m}',\bar{n}' = 1,2,3,\cdots M,N$$
$$p,q,\bar{p},\bar{q},p',q',\bar{p}',\bar{q}' = 1,2,3,\cdots P,Q \quad (32)$$

with

$$E^{rs}_{im} = \int_{-1}^{1}\left[\frac{d^r\phi_i(\xi)}{d\xi^r}\frac{d^s\phi_m(\xi)}{d\xi^s}\right]d\xi;$$
$$F^{rs}_{jn} = \int_{-1}^{1}\left[\frac{d^r\varphi_j(\eta)}{d\eta^r}\frac{d^s\varphi_n(\eta)}{d\eta^s}\right]d\eta \quad (33)$$

and the components of in-plane stiffness $A^c_{ij}=A^{(1)}_{ij}$, $A^f_{ij}=A^{(2)}_{ij}=A^{(3)}_{ij}$; bending-stretching coupling stiffness $B^c_{ij}=B^{(1)}_{ij}=0$, $B^f_{ij}=B^{(2)}_{ij}=-B^{(3)}_{ij}$; and bending stiffness $D^c_{ij}=D^{(1)}_{ij}$, $D^f_{ij}=D^{(2)}_{ij}=D^{(3)}_{ij}$.

References

ANSYS. (1997). *The ANSYS release 5.4 user's manual*, ANSYS Inc., Canonsburg, Pa.

ASTM. (1990). *Standards and literature references for composite materials*, 2nd Ed., West Conshohocken, Pa.

Berman, A., and Nagy, E. J. (1983). "Improvement of a large analytical model using test data." *AIAA J.*, 21, 1168–1173.

Castagnède, B., Jenkins, J. T., Sachse, W., and Baste, S. (1990). "Optimal determination of the elastics constants of composite materials from ultrasonic wave-speed measurements." *J. Appl. Phys.*, 67, 2753–2761.

Deobald, L. R., and Gibson, R. F. (1988). "Determination of elastic constants of orthotropic plates by a modal analysis/Rayleigh-Ritz technique." *J. Sound Vib.*, 124(2), 269–283.

Fallstrom, K. E., and Jonsson, M. (1991). "A nondestructive method to determine material properties in anisotropic plate." *Polym. Compos.*, 12(5), 293–305.

Hwang, S. F., and Chang, C. S. (2000). "Determination of elastic constants of materials by vibration testing." *Compos. Struct.*, 49, 183–190.

IMSL. (1991). *IMSL MATH/LIBRARY*, 2nd Ed., IMSL, Inc., Houston.

Kam, T. Y., and Jan, T. P. (1995). "First-ply failure analysis of laminated composite plates based on the layerwise linear displacement theory." *Compos. Struct.*, 32(4), 583–591.

Kam, T. Y., and Lee, T. Y. (1994). "Crack size identification using and expanded mode method." *Int. J. Solids Struct.*, 31, 925–940.

Kam, T. Y., and Liu, C. K. (1998). "Stiffness identification of laminated composite shafts." *Int. J. Mech. Sci.*, 40(9), 927–936.

Lauwagie, T., Sol, H., and Heylen, W. (2006). "Handling uncertainties in mixed numerical–experimental techniques for vibration based material identification." *J. Sound Vib.*, 291(3-5), 723–739.

Masoud, R. R., and Pierre, M. (1999). "Buckling and vibration analysis of composite sandwich plates with elastic rotational edge restraints." *AIAA J.*, 37(5), 579–587.

Mau, S. T. (1973). "A refined laminate plate theory." *J. Appl. Mech.*, 40, 606–607.

Moussu, F., and Nivoit, M. (1993). "Determination of elastic constants of orthotropic plates by a modal analysis/method of superposition." *J. Sound Vib.*, 165(1), 149–163.

Nayak, A. K., Moy, S. S., and Shenoi, R. A. (2002). "Free vibration analysis of composite sandwich plates based on Reddy's higher-order theory." *Composites, Part B*, 33, 505–519.

Qian, G. L., Hoa, S. V., and Xiao, X. (1997). "A vibration method for measuring mechanical properties of composite, theory and experiment." *Compos. Struct.*, 39(1-2), 31–38.

Saito, T., Parbery, R. D., Okuno, S., and Kawano, S. (1997). "Parameter identification for aluminum honeycomb sandwich panels based on orthotropic Timoshenko beam theory." *J. Sound Vib.*, 208(2), 271–287.

Snyman, J. A., and Fatti, L. P. (1987). "A multistart global minimization algorithm with dynamic search trajectories." *J. Optim. Theory Appl.*, 54(1), 121–141.

Sol, H., Hua, J., Visscher, J., Vantomme, J., and Wilde, W. P. (1997). "A mixed numerical/experimental technique for the nondestructive

J. Eng. Mech. 2007.133:874-886.

identification of the stiffness properties of fiber reinforced composite materials." *NDT & E Int.*, 30(2), 85–91.

Swanson, S. R. (1997). *Introduction to design and analysis with advanced composite materials*, Prentice-Hall, Upper Saddle River, N.J.

Thwaites, S., and Clark, N. H. (1995). "Nondestructive testing of honeycomb sandwich structures using elastic waves." *J. Sound Vib.*, 187(2), 253–269.

Ueng, C. E. S. (1966). "Natural frequencies of vibration of an all-clamped rectangular sandwich panel." *J. Appl. Mech.*, 33(3), 683–684.

Vanderplaats, G. N. (1984). *Numerical optimization techniques for engineering design with applications*, McGraw-Hill, New York, Chap. 5.

Wang, W. T., and Kam, T. Y. (2001). "Elastic constants identification of shear deformable laminated composite plates." *J. Eng. Mech.*, 127(11), 1117–1123.

Watanabe, N., Miyachi, K., and Daimon, M. (1993). "Stiffness and vibration characteristic of sandwich plates with anisotropic composite laminates face sheets." *Proc., Conf. on AIAA/ASME/ASCE/AHS/ASC 34th Structures, Structural Dynamics, and Material*, 236–244.

J. Eng. Mech. 2007.133:874-886.